El Gharamti, Iman; Dempsey, John; Polojärvi, Arttu; Tuhkuri, Jukka

Fracture and Creep of Warm and Floating Columnar Freshwater Ice Under Different Loading Scenarios Under Laboratory Conditions

Published in:
Proceedings of the 26th IAHR International Symposium on Ice

Published: 01/01/2022

Document Version
Publisher's PDF, also known as Version of record

Please cite the original version:
El Gharamti, I., Dempsey, J., Polojärvi, A., & Tuhkuri, J. (2022). Fracture and Creep of Warm and Floating Columnar Freshwater Ice Under Different Loading Scenarios Under Laboratory Conditions. In *Proceedings of the 26th IAHR International Symposium on Ice* (IAHR International Symposium on Ice). International Association for Hydro-Environment Engineering and Research.

IAHR AIRH

26th IAHR International Symposium on Ice
Montréal, Canada – 19-23 June 2022

Fracture and Creep of Warm and Floating Columnar Freshwater Ice Under Different Loading Scenarios in the Aalto Ice Tank

Iman E. Gharamti[*], John P. Dempsey[#], Arttu Polojärvi[*], Jukka Tuhkuri[*]
[*]Department of Mechanical Engineering, Aalto University, Espoo 00076, Finland
[#]Department of Civil and Environmental Engineering, Clarkson University, Potsdam, NY 13699, USA
e-mail: iman.elgharamti@aalto.fi, jdempsey@clarkson.edu, arttu.polojarvi@aalto.fi, jukka.tuhkuri@aalto.fi

Investigating the mechanics of freshwater ice fracture is crucial for ensuring safe activities in lakes and rivers. Climate change is bringing warmer conditions and making the ice warmer. Accordingly, the necessity to study and model warm ice is increasing. The properties and behavior of the ice may be fundamentally different when it is warm, very close in temperature to zero degrees, than cold. While cold ice has been mainly studied in the literature, this paper reviews a study case of warm freshwater ice (>-0.5ºC) and provides a strong evidence that warm ice may behave differently than the cold ice typically tested in laboratories or nature. Large-scale fracture experiments, using edge-cracked rectangular plates loaded at the crack mouth, were conducted in the Ice Tank of Aalto University. The plates covered a size range of 1:39, the largest for ice tested under laboratory conditions, with three plate sizes: 0.5m x 1m, 3m x 6m and 19.5m x 36m. The monotonic loading rates applied led to test durations from fewer than 2 seconds to more than 1000 seconds, with some experiments tested under creep/cyclic-recovery loading. Under the monotonic loading, size and rate effects were interrelated as rate dependent size effects and size dependent rate effects. Under the creep/cyclic-recovery conditions, the way the ice deformed did not fit our conventional understanding, and the ice response was interestingly elastic-viscoplastic with no significant viscoelasticity.

1. Introduction

Global warming is bringing new conditions to the Arctic and Antarctic environments. The ice is becoming warmer, thinner, weaker, and fragmented. These tremendous changes necessitate a better understanding of the physics and mechanics of the new ice. Historically, cold ice has been studied typically. The properties and behavior of the ice may be fundamentally different when it is warm, very close in temperature to zero degrees, than cold. It is crucial to build a fundamental knowledge of warm ice on the basis of scientific and experimental investigation. Only then, we can build well-validated physical models that can predict the ice-induced loads and eventually ensure the safety of operations in ice-covered areas.

The deformation and fracture processes of freshwater ice are important in many engineering applications. For example, freshwater ice sheets fracture when in contact with ships, river ice breaks up during interaction with bridge piers, and thermal cracks form in lakes and reservoirs. In fact, warming of the ice increases the importance of creep deformations, which must be modeled in order to obtain the true fracture behavior. Another aspect of the ice behavior, which should be examined and modeled, is the dependency on many factors: temperature, strain rate, scale, microstructure, etc. That being said, a reliable fracture model of ice should capture the time-dependent behavior of ice as well as the interrelation of the different influencing factors.

This paper reviews a set of fracture and creep experiments of warm columnar freshwater ice (>-0.5^{o}C) and provides a strong evidence that warm ice may behave differently than the cold ice typically tested in laboratories or nature. Large-scale fracture experiments, using edge-cracked rectangular plates (ECRP) loaded at the crack mouth, were conducted in the Ice Tank of Aalto University. The plates covered a size range of 1:39, the largest for ice tested under laboratory conditions, with three plate sizes: 0.5m x 1m, 3m x 6m and 19.5m x 36m. The test program was divided into two parts. In the first part, fourteen tests were conducted in displacement control (DC) with the three plate sizes and loaded with different rates monotonically to fracture. In the second part, five tests of 3m x 6m ECRP were loaded in load control (LC) under creep-recovery loading and monotonic loading to fracture. Creep and cyclic sequences were applied maintaining peak loads well below the failure loads, followed by monotonic ramps leading to complete fracture of each specimen. Full details of the DC and LC analysis and modelling are provided in (Gharamti et al 2021a) and (Gharamti et al 2021b), respectively. This paper focuses on summarizing merely the experimental results.

The rest of the paper is structured as follows. In Section 2, descriptions of the ice growth and the ice characterization are presented. Section 3 presents the experimental setup and explains the different loading scenarios. The experimental results for the DC and LC tests are given in Section 4 and discussed in Section 5. The paper ends with a conclusion.

2. Ice Growth and Characterization

A 40m x 40m sheet of columnar freshwater S2 ice was grown in the Ice Tank of Aalto University. The growth process was initiated by lowering the air temperature in the ice tank to -14^{o}C. A fine mist of water droplets, at around 2^{o}C, was sprayed into the air above the basin. Once the droplets reached the water surface, they acted as nuclei for ice crystals to form. After four weeks at -14^{o}C, the initial seeded ice layer developed into a sheet of columnar S2 ice with a thickness of approximately 34 cm. For the experiments, the ambient temperature was raised to -2^{o}C and maintained at that temperature. The ice thickness was homogeneous but increased from 34 cm to 41 cm during the test program that lasted a few

weeks. The ice thickness at the crack tip (h) was measured before each test and is reported in Table 1. The ice was warm (>-0.5°C, Fig. 1a) with a near-linear temperature gradient.

The microstructure of the ice was analyzed by making thin sections in a cold room. The conventional way of thinning ice with a microtome was replaced by a milling machine (Fig. 2a), which proved to be very efficient and fast. The thin sections were then examined and photographed under cross-polarized light.

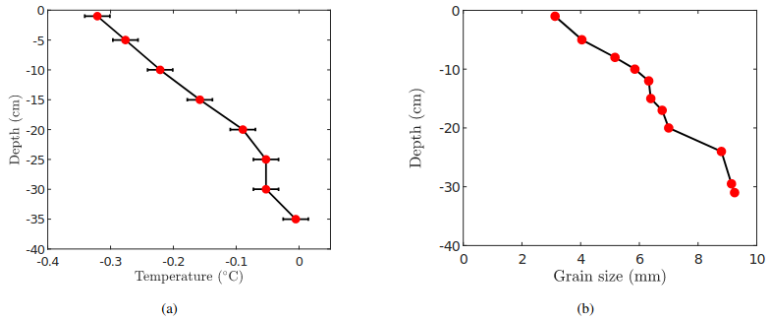

Figure 1. (a) Temperature profile. Each data point represents the average of measurements taken at the same depth of different ice cores throughout the one month duration of the test program. (b) Grain size distribution. Each data point is measured from one thin section (Gharamti et al. 2021b).

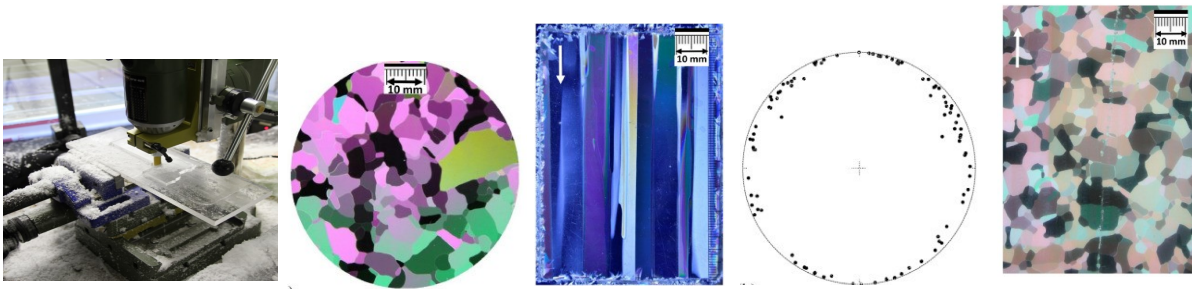

(a) (b) (c) (d) (e)

Figure 2. (a) Producing thin sections using a milling machine. (b) Horizontal thin section taken from the middle of the ice sheet and (d) its corresponding c-axis orientation Shmidt net. (c) Vertical thin section showing columnar freshwater ice at the bottom of the ice sheet. The arrow indicates the growth direction. (e) Horizontal thin section showing a crack path and taken from a depth of 24 cm from the top of the ice sheet. The arrow indicates the direction of crack propagation (Gharamti et al. 2021a, 2021d).

Figs. 2b and 2c show horizontal and vertical sections, respectively, displaying the crystalline and columnar structure of the ice. The grain size varied between 3 mm at the top and 10 mm at the bottom portion of the ice sheet, with an average size of 6.5 mm (Fig. 1b). An examination of the c-axis orientation was carried out by analyzing hundreds of grains at different locations and depths along the ice sheet. The c-axis orientation plot from horizontal thin section (Fig. 2b) taken from the middle of the ice sheet is shown in Fig. 2d. The Schmidt net consists of 100 poles of the basal planes measured with a four-axis universal Rigsby stage. In the type of axis projection plot used (Langway 1958), a horizontal c-axis would be on the circumference and a vertical c-axis would be at the center. It can be seen that the c-axes of the columnar grains were randomly horizontal. The ice sheet had the same type of textural features throughout the depth and for the whole ice sheet: the ice was columnar freshwater S2 ice.

3. Description of the Experiments

A deeply cracked edge-cracked rectangular plate (ECRP) configuration, of width H and length L, loaded at the crack mouth was used ($H = 2L$, Fig. 3a).

Three specimen sizes were cut from the parent sheet, 0.5m x 1m, 3m x 6m and 19.5m x 36m, covering a size range of 1:39, which is the largest for ice under laboratory conditions. A long tip-sharpened edge crack of length A_0 (A_0 = 70-75% L, Fig. 3a) was cut in each ice specimen.

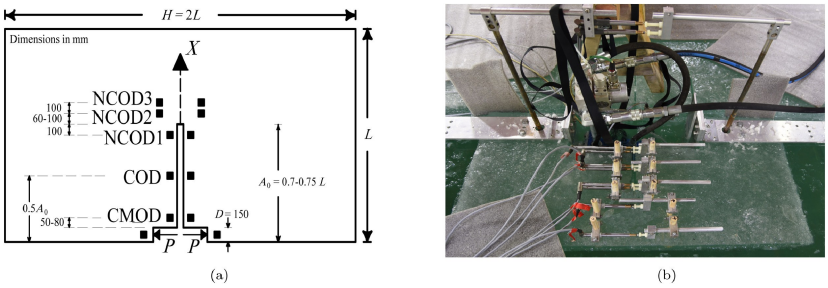

Figure 3. (a) Specimen geometry, edge cracked rectangular plate of length L, width H, and crack length A_0. (b) In-situ experimental setup of a 0.5m x 1m ice specimen (Gharamti et al. 2021c)**.**

The crack opening displacement was monitored at different positions along the crack by using surface-mounted linear variable differential transducers (LVDTs), labelled in Fig. 3a as CMOD (at the crack mouth), COD (midway of the crack), NCOD1 (10 cm behind the tip), NCOD2 (6–10 cm ahead of the tip), and NCOD3 (20 cm ahead of the tip). A hydraulically operated closed-loop device was inserted in the crack mouth to load the specimen, with a contact loading length of 150 mm, denoted by D in Fig. 3a. Fig. 3b shows the in-situ experimental setup of a 0.5m x 1m specimen.

A total of 19 tests were completed. Fourteen tests were conducted in displacement control (DC) and loaded with different rates monotonically to fracture. The plates covered the three plate sizes. The monotonic loading rates applied led to test durations from fewer than 2 seconds to more than 1000 seconds. Five tests of 3m x 6m ECRP were loaded in load control (LC) under creep-recovery loading and monotonic loading to fracture. Creep and cyclic sequences were applied maintaining peak loads well below the failure loads, followed by monotonic ramps leading to complete fracture of each specimen (Fig. 4). Fig. 2e shows that transgranular fracture was dominant: the cracks propagated through the grain for almost all the grains and straight through NCOD2 and NCOD3 to the far plate edge (Fig. 3a).

4. Results

4.1. DC Monotonic Tests

Table 1 gives the dimensions of the ice samples together with the measured and computed results. P_{max} is the peak or failure load. The apparent fracture toughness (K_Q) was computed from the failure load and dimensions using Eq. (1) in (Gharamti et al. 2021a). The loading rate ($\dot{K}$) was computed by dividing K_Q by the time to failure (t_f). The time to failure varied from about 2 seconds to about 1000 seconds giving a loading rate range of 0.18-57 kPa$\sqrt{m}s^{-1}$. Displacements at the crack mouth and near the crack tip at the crack growth initiation, CMOD and NCOD1 respectively, were measured at locations shown in Fig. 3. $\dot{CMOD}$ and $\dot{NCOD}1$ indicate the displacement rates and were obtained by dividing CMOD and NCOD1 by the time to failure.

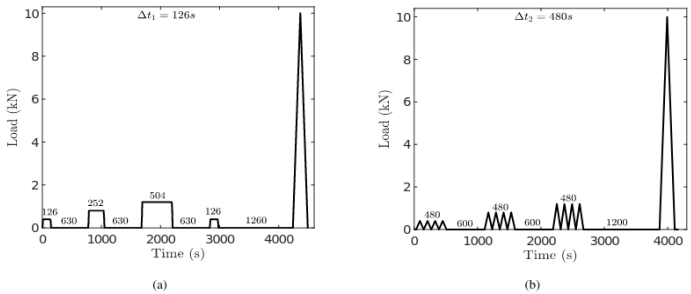

Figure 4. Loading consisting of (a) creep-recovery and (b) cyclic sequences followed by a monotonic fracture ramp. The number above each segment indicates the duration in seconds (Gharamti et al. 2021b).

Table 1. DC tests: specimen dimensions, measured data, and results computed using linear elastic fracture mechanics (Gharamti et al. 2021a)

Test	L m	H m	A_0 m	h cm	P_{max} kN	t_f s	K_Q kPa$\sqrt{\text{m}}$	$\dot{K}$ kPa$\sqrt{\text{m}}$s^{-1}	CMOD μm	$\dot{\text{CMOD}}$ μms^{-1}	NCOD1 μm	$\dot{\text{NCOD1}}$ μms^{-1}
RP1	0.5	1	0.35	35	1.7	54.9	126.2	2.298	33.1	0.602	5.2	0.094
RP2	0.5	1	0.35	35	2.3	51.9	168.6	3.247	43.3	0.834	7.5	0.145
RP3	0.5	1	0.35	37.1	1.6	1.9	108.4	57.058	29.1	15.321	7.8	4.128
RP4	0.5	1	0.35	37.6	1.9	20.8	129.2	6.223	37.6	1.811	3.2	0.154
RP5	0.5	1	0.35	40.2	2.1	571.7	132.2	0.231	36.1	0.063	3.4	0.006
RP6	0.5	1	0.35	41.1	2.4	811.4	145	0.179	59.5	0.073	10.4	0.013
RP7	3	6	2.1	34.5	4.6	86.9	159.4	1.834	236	2.716	47.2	0.543
RP8	3	6	2.1	34.5	3.0	2.7	106	39.259	157	58.148	22.9	8.482
RP9	3	6	2.1	34.5	5.2	148.0	180.6	1.221	266	1.798	42.8	0.289
RP10	3	6	2.1	34.5	4.8	222.2	166.8	0.751	215.6	0.970	34.6	0.156
RP11	3	6	2.1	36	4.2	15.3	139.4	9.091	174.4	11.374	25.2	1.644
RP12	3	6	2.1	37.2	6.8	701.8	221.3	0.315	370.5	0.528	68.5	0.098
RP13	3	6	2.1	37.6	5.7	1027.1	184.3	0.179	420.3	0.409	63.4	0.062
RP14	19.5	36	14.6	35	10	213.5	186.0	0.871	961.7	4.505	37.2	0.174

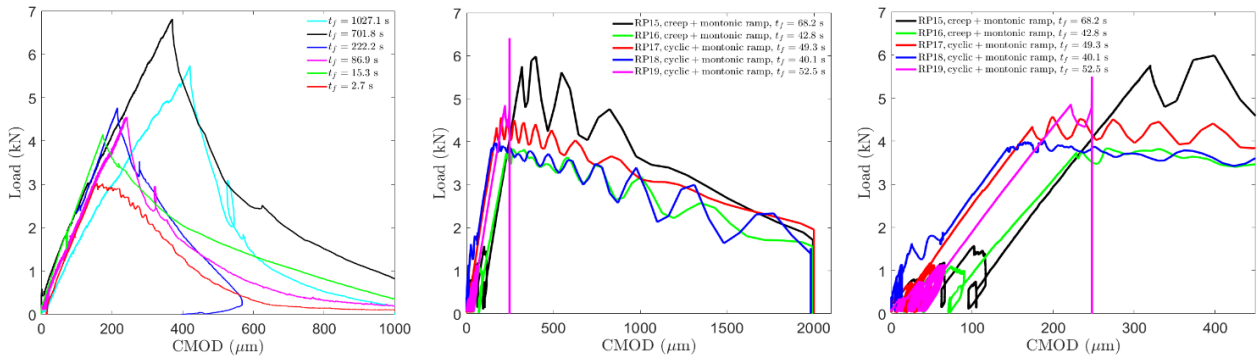

Figure 5. Measured load versus CMOD for the (a) DC tests, (b) LC tests, and (c) LC tests up to the peak load (Gharamti et al. 2021b).

Fig. 5a shows the load-CMOD records for the 3m x 6m specimens. The peak load decreased with the increase in the loading rate. The load-displacement relation up to the peak load is linear at high loading rates, but non-linear at low loading rates.

Fig. 6 shows the apparent fracture toughness (K_Q) and near-crack-tip opening displacements (NCOD1) at the crack growth initiation as functions of loading rate. Interestingly, the data suggests an interrelated rate and size effects that can be interpreted in two ways: 1) Loading rate dependent size effect: there is a size effect at low rates, but there is no size effect at high

rates. At low rates, K_Q and NCOD1 are higher for the large specimens (both 3m x 6m and 19.5m x 36m) than for the small specimens (0.5m x 1m), but with increasing loading rate, the specimen size does not have an effect on K_Q, and NCOD1 for the large specimen approaches the NCOD1 of the small specimen.

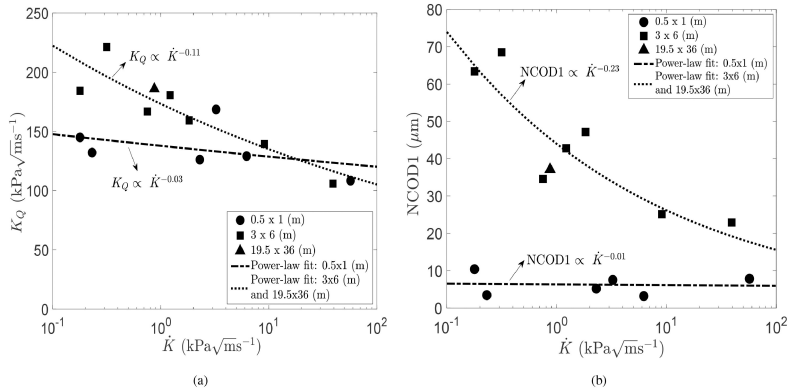

Figure 6. Measured apparent fracture toughness (a) and near-crack-tip opening displacements (b) as a function of loading rate. First-order power-law fits were applied separately for the larger specimen (3m x 6m and 19.5m x 36m) and for the smaller specimen (0.5m x 1m) (Gharamti et al. 2021a).

2) Size dependent rate effect: for both the large and small specimens, K_Q and NCOD1 are decreasing with increasing loading rate, but this rate effect is stronger for the large specimens. This observed size effect is clear between specimens of size 0.5m x 1m and of size 3m x 6m, but there was no size effect between the 3m x 6m specimens and the largest specimen of size 19.5m x 36m.

4.2. LC Creep/Cyclic-Recovery Tests

Table 2. LC tests: Measured experimental data and computed results (Gharamti et al. 2021b)

Test	Type	L (m)	H (m)	A_0 (m)	h (mm)	$P_{\max}$ (kN)	t_f (s)	CMOD (μm)	$\dot{\text{CMOD}}$ (μms^{-1})	NCOD1 (μm)	$\dot{\text{NCOD1}}$ (μms^{-1})
RP15	creep	3	6	2.1	364	5.8	68.2	320.1	4.7	53.6	0.8
RP16	creep	3	6	2.1	385	3.8	42.8	228.2	5.3	49.1	1.1
RP17	cyclic	3	6	2.1	407	4.5	49.3	173.7	3.5	30.0	0.6
RP18	cyclic	3	6	2.1	408	3.9	40.1	143.7	3.6	28.5	0.7
RP19	cyclic	3	6	2.1	412	6.3	52.5	221.4	4.2	44.0	0.8

Table 2 shows the measured and computed parameters for the LC experiments. Fig. 7 gives the results of the peak load $P_{\max}$, crack mouth opening displacement CMOD, and near crack-tip opening displacement NCOD1 as a function of the loading time for the 3m x 6m specimens of the DC and LC tests. First-order power-law fits were applied to the data of the DC tests. The LC values lie above, below, and along the DC fit. No clear effect of creep and cyclic loading on the fracture properties was detected.

Fig. 5b show the experimental load versus the crack opening displacement at the crack mouth for LC tests, respectively. Fig. 5c displays a zoomed view of the fracture ramp of the LC tests. Comparing the failure loads of the DC (Fig. 5a) and LC tests indicates that the failure

loads, of tests with comparable loading rates, were similar. The gradual decay of the load portrays the time dependency in the behavior of freshwater ice.
Fig. 8 shows the experimental results for RP16: the applied load and the crack opening displacements at the crack mouth (CMOD), halfway of the crack (COD), and 10 cm behind the tip (NCOD1) (Fig. 3a). Similarly, Fig. 9 shows the experimental response for RP17. The time-dependent nature of of the ice response is evident.

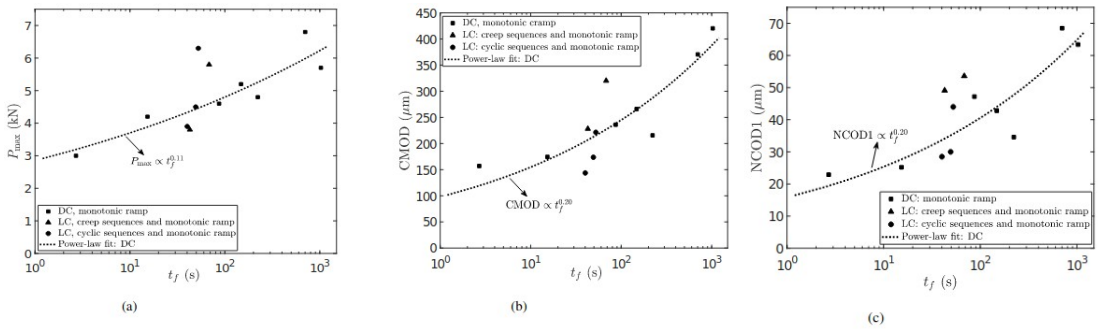

Figure 7. Experimental results for the (a) peak load P_{max}, (b) crack mouth opening displacement CMOD and (c) near crack tip opening displacement NCOD1 at crack growth initiation, as a function of time to failure t_f for the DC and LC tests (Gharamti et al. 2021b).

It is clear from Figs. 8b and 9b that the CMOD, COD, and NCOD1 displacements were composed mainly of elastic and viscoplastic components. No significant viscoelasticity was detected in the displacement-time records for all the tests. The displacement-time slope was linear and constant, indicating that the primary (transient) creep stage is almost absent or instantaneous and the secondary/steady-state creep regime is dominant during each load application. The recovery phases consisted mainly of an elastic recovery (instantaneous drop) and unrecovered viscoplastic displacement. The behavior as observed resembles the response of a Maxwell model composed of a series combination of a nonlinear spring and nonlinear dashpot (Fig. 8d).

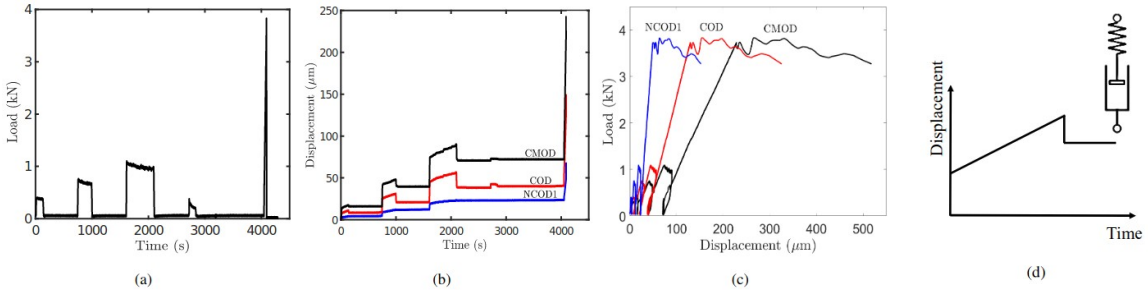

Figure 8. Experimental results for RP16. (a) Load at the crack mouth. (b) Displacement - time records. (c) Load – displacement record. (d) Typical response of a Maxwell model, consisting of a nonlinear spring and nonlinear dashpot, to a constant load step (Gharamti et al. 2021b).

5. Discussion

5.1. DC Monotonic Tests

The fracture experiments conducted with columnar freshwater S2 ice showed both size and rate effects which can be expressed either as a rate dependent size effect or as a size

dependent rate effect. There was a size effect at the lower rates but no size effect at the higher rates. There was a rate effect for the larger specimens but a weak or no rate effect for the smaller specimens. This interrelation of size and rate effects for columnar freshwater ice is a novel observation; earlier experiments, summarized in (Gharamti et al. 2021a) have observed rate effects or size effects, but not how these two are related. Compared with the earlier studies with freshwater S2 ice, the specimens tested here were large (L ≥ 0.5)m, very warm (>−0.5 °C), and tested in-situ.

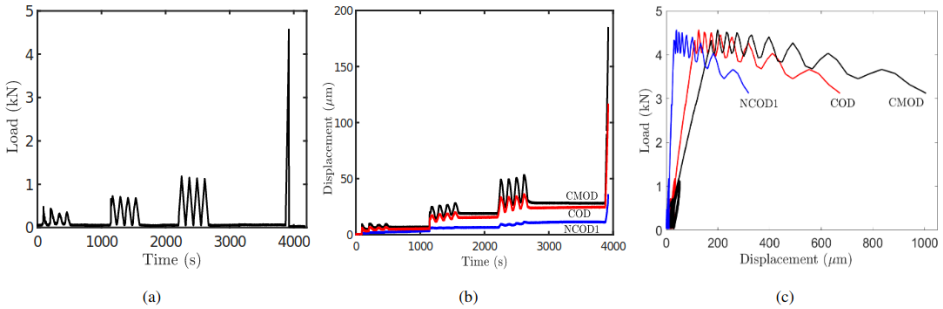

Figure 9. Experimental results for RP17. (a) Load at the crack mouth, see Fig. 3a. (b) Displacement - time records. (c) Load – displacement record (Gharamti et al. 2021b).

The apparent fracture toughness (K_Q) measured (about 100 kPa√m at high rates and about 100−200 kPa√m at low rates) is within the range measured earlier for columnar S2 freshwater ice (Bentley et al. 1989, Dempsey 1991). While values for K_Q are given in Table 1 and Fig. 6a, the validity of K_Q as a material parameter for ice requires rethinking the corresponding assumptions (Dempsey 2018). K_Q is a linear elastic fracture mechanics parameter (LEFM) and thus limited to be used when the material response can be idealized as linearly elastic, except in a small process zone near the crack tip. Instead, Gharamti et al. (2021a) applied a viscoelastic fictitious crack model which proved successful in analyzing the fracture of freshwater ice and modeling the experimental data.

The results of the two larger, 3m x 6m and 19.5m x 36m, samples were interchangeable suggesting that the 3m x 6m sample size is large enough to give size-independent fracture results for this type of warm ice. Accordingly, the following requirement can be recommended to satisfy polycrystalline homogeneity.

$$L/d_{av} \geq 460 \qquad \textbf{[1]}$$

in which L is the specimen size in the cracking direction (Fig. 3a) and d_{av} is a measure of the average grain size (Fig. 1b).

5.2. LC Creep/Cyclic-Recovery Tests

The creep and cyclic sequences preceding the fracture ramp did not affect the fracture behavior: failure load and crack opening displacements at crack growth initiation.

The observed elastic-viscoplastic response is a novel result for any type of ice. This behavior differs from previous experimental creep and cyclic work, discussed by Gharamti et al. (2021b), on freshwater ice. Viscoelasticity normally results from the elastically-accommodated grain boundary sliding upon unloading. During loading, internal stresses develop at local stress concentrations in the grain boundary geometry (triple points and grain boundary ledges). Assuming there is no microcracking, the growing stress impedes further grain boundary sliding and causes sliding in the reverse direction, giving rise to the

recoverable component after unloading. However, in the present case, the viscoelastic deformation was overall absent.

Several reasons can be discussed, related to the ice temperature, microstructure, and nonlinear mechanisms in the process zone: 1) Concerning the effect of temperature, the warmer the ice temperature, the more liquid on the grain boundary (Dash et al. 2006). The intergranular melt phase on the grain boundary renders the ice as two-phase polycrystal and significantly influences the creep and recovery response. In fact, the grain boundary sliding then consists theoretically of two processes: a) the sliding of grains over one another and b) the squeezing-in/out of the liquid between adjacent grains (Muto and Sakai 1998). The shear behavior of the liquid film is function of its properties (thickness and amount). This liquid phase acts as a resisting obstacle for the grains to shear and deform back to their original form, causing the viscoplastic deformation. 2) The microstructure (grain size, crystalline texture) could be another contributing factor. Sinha (1979) concluded that delayed elastic strain exhibits an inverse proportionality with grain size. This suggests that the grain size (3-10 mm, Fig. 1b) of the ice samples is coarse enough not to produce any measurable viscoelastic deformation under the testing conditions. It is also probable that for this grain size, there was not enough local concentration points to arrest the grain boundary sliding and drive the recoverable and reverse sliding. 3) Gasdaska (1994) discussed that regularly ordered and packed microstructures limit the amount of sliding and rearrangement and lead to less anelastic strain. The ice growth in the Aalto Ice tank was very controlled and resulted in homogeneous ice sheet. 4) Knauss (2015) presented a thorough review of the time-dependent fracture models available to date. The essence of the models is based on modelling the behavior in a finite cohesive/process zone which is attached to the traction-free crack tip. It is believed that the mechanisms taking place in the process zone play an influencing role in the current tests. The nonlinearity in the fracture zone relieved the internal stresses that would ordinarily accommodate the grain boundary sliding and generate some viscoelastic deformation upon unloading. Thus, any microstructural damage that occurred during loading manifested as permanent deformation at the end of the test.

All the above-mentioned factors might have contributed to the measured elastic-viscoplastic response. However, the question as to which factor influenced mostly the behavior requires more testing programs that examines the effect of each factor separately.

6. Conclusion

This paper examined the fracture behavior of warm and floating columnar freshwater S2 ice under different loading (monotonic, creep, cyclic) scenarios, by varying the specimen size and loading rate/type in an in-situ experimental program.

Fourteen DC monotonic experiments on size (scale) and rate effects were completed. The ECRP covered a size range of 1:39; the largest sample had dimensions of 19.5mx36m. The main observation from the experiments is that the size and rate effects were interrelated. This can be interpreted as rate dependent size effects; there was a size effect at low loading rates, but no size effect was observed at the higher rates. This interrelation can be expressed also as size dependent rate effects. For the larger specimen (3m x 6m and 19.5m x 36m), a clear rate effect was observed, while for the small specimen (0.5m x 1m) the rate effect was weak or absent. The results of the two larger, 3m x 6m and 19.5m x 36m, samples were interchangeable suggesting that the 3m x 6m sample size is large enough to give size-independent fracture results for this type of warm ice.

Five LC creep/cyclic-recovery experiments on the time-dependent deformation were completed. The results showed that the creep and cyclic sequences had no clear effect on the failure load and the crack opening displacements at crack growth initiation. The way the ice deformed did not fit our conventional understanding, and the ice response was interestingly elastic-viscoplastic with no significant viscoelasticity.

Overall, the paper provides a strong evidence that warm ice may behave differently than cold ice. This is a very significant scientific result and calls for further research, to study systematically the parameters that affect ice deformation close to the melting point. This is also very timely: We need to know what happens when global warming brings new conditions. It looks like the old rules may not hold up.

Acknowledgments
This work was funded though the Finland Distinguished Professor programme "Scaling of Ice Strength: Measurements and Modeling", and through the ARAJÄÄ research project, both funded by Business Finland and the industrial partners Aker Arctic Tech-405 nology, Arctech Helsinki Shipyard, Arctia Shipping, ABB Marine, Finnish Transport Agency, Suomen Hyötytuuli Oy, and Ponvia Oy. This financial support is gratefully acknowledged.

References

Gharamti, I. E., Dempsey, J. P., Polojärvi, A., & Tuhkuri, J., 2021a. Fracture of warm S2 columnar freshwater ice: size and rate effects. *Acta Materialia*, 202, p. 22-34.

Gharamti, I. E., Dempsey, J. P., Polojärvi, A., & Tuhkuri, J., 2021b. Creep and fracture of warm columnar freshwater ice. *The Cryosphere*, *15*(5), p. 2401-2413.

Gharamti, I. E., Dempsey, J. P., Polojärvi, A., & Tuhkuri, J., 2021c, Fracture energy of columnar freshwater ice: Influence of loading type, loading rate and size. *Materialia*, 20, 101188.

Gharamti, I. E., 2021d, Rate and Size Effects on the Deformation and Fracture of Warm and Floating Columnar Freshwater Ice, PhD Thesis, Aalto University.

Langway, C. C., 1958, Ice fabrics and the universal stage. CRREL Technical Report 62.

Sinha, N. K., Ehrhart, P., Carstanjen, H., Fattah, A., and Roberto, J., 1979, Grain boundary sliding in polycrystalline materials, Philosophical Magazine A, 40, p. 825–842.

Knauss, W. G., 2015, A review of fracture in viscoelastic materials, International Journal of Fracture, 196, p. 99–146.

Gasdaska, C. J., 1994, Tensile creep in an in situ reinforced silicon nitride, Journal of the American Ceramic Society, 77, p. 2408–2418.

Dempsey, J. P., Cole, D. M., and Wang, S., 2018, Tensile fracture of a single crack in first-year sea ice, Philosophical Transactions of the Royal Society A, 376, 20170346.

Dempsey, J. P., 1991, The fracture toughness of ice, Ice-Structure Interaction, Springer, Berlin, Heidelberg, p. 109-145

Dash, J., Rempel, A., and Wettlaufer, J., 2006, The physics of premelted ice and its geophysical consequences, Reviews of modern physics, 78, 695.

Muto, H. and Sakai, M.: Grain-boundary sliding and grain interlocking in the creep deformation of two-phase ceramics, Journal of the American Ceramic Society, 81, 1611–1621, 1998.

Bentley, D.L., Dempsey, J.P., Sodhi, D.S. and Wei, Y., 1989. Fracture toughness of columnar freshwater ice from large scale DCB tests. *Cold regions science and technology*, *17*(1), pp.7-20.